

# A simplified compression test for the estimation of the Poisson's ratio of viscoelastic foams

Paolo Bonfiglio<sup>1</sup>, Francesco Pompoli<sup>1</sup>

<sup>1</sup> Dipartimento di Ingegneria, Università degli Studi di Ferrara

Via Saragat 1, 44122 Ferrara, ITALY

Corresponding author

Paolo Bonfiglio

Dipartimento di Ingegneria, Università degli Studi di Ferrara, Via Saragat 1, 44122  
Ferrara, ITALY

Tel.:+390532974876

[paolo.bonfiglio@unife.it](mailto:paolo.bonfiglio@unife.it)

## **Abstract**

This paper describes a simplified procedure for determining the Poisson's ratio of homogeneous and isotropic viscoelastic materials. A cylindrical shaped material is axially excited by an electromagnetic shaker and consequent displacement waves are investigated. Using a frequency sweep as an excitation signal, the frequency domain displacement response is measured upstream and sideways of the sample itself. A plane cross-section analytical model of the experimental setup is used to estimate Poisson's ratio through a minimization-based procedure, applied to radial displacement once the complex modulus has been directly determined under the assumption of spring-like behaviour of the axial displacement. The results are presented and discussed for different materials and compared to well-established quasi-static and finite element simulations.

**Keywords:** viscoelastic materials, Poisson's ratio, measurement methods

## 1. INTRODUCTION

Poisson's ratio can play a relevant role in characterizing the linear dynamic behavior of viscoelastic materials for noise and vibration control. In addition, this parameter occurs in several equations to be solved within the context of analytical and numerical (finite element method, statistical energy analysis, transfer matrix method) simulations. Poisson's ratio is defined as the ratio of lateral strain to axial strain in an axially loaded linear elastic solid, and this ratio is a real number in case of ideal elasticity. In contrast, in viscoelastic materials, as a result of damping, this ratio can be considered as a complex number [1-2]. However, several studies [3-4] have demonstrated that a real valued and frequency-independent Poisson's ratio can provide reliable results and can be considered a good enough approximation when the aim is to calculate main vibro-acoustical indicators (dynamic stiffness, sound absorption, sound transmission loss, etc...).

In literature several methods (direct and indirect) have been proposed for determining mechanical parameters of materials for vibration and noise control applications, and a comprehensive review is discussed in ref. [5]. As stated in ref. [2], while a lot of research has been proposed for the measurement of complex moduli, fewer experimental works have focused on determining Poisson's ratio. Recently, methods based on digital image correlation (DIC) through uniaxial relaxation tests [6] and empirical correlation between hardness and elastic moduli, along with the usual instrumented indentation test [7] have been proposed in literature for characterizing the Poisson's ratio polymeric and composite materials. Although both methods can give a reliable estimation of Poisson's ratio they have been applied to material having an hardness which is too high if compared with foams used in noise and vibration control applications.

The aim of this research is to present a method to determine Poisson's ratio (real valued and frequency independent), through measuring the radial displacement of a cylinder of homogeneous and isotropic material at low frequencies, once the complex modulus has been determined in advance, using a transfer matrix approach, as described in ref. [8]. In particular, an analytical model for axial and radial displacement, based on the Mindlin-Hermann two modes theory [9], has been applied and an estimation of Poisson's ratio can be easily obtained by minimizing the difference between experimental and numerical radial displacement in the frequency domain. Measurement and analyses are limited in a frequency range where all tested samples are much smaller than the longitudinal wavelength.

The paper is organised as follows. Section 2 contains a description of methodology. A description of the experimental set-up and tested materials is provided in Section 3. Section 4 contains analytical model validation, results obtained using the proposed methodology, and a comparison of different measurement techniques. The last section contains concluding remarks.

## 2. DESCRIPTION OF METHODOLOGY

### 2.1. Theoretical background

Consider a solid, elastic, isotropic cylinder of finite length  $L$  and radius  $R$ , as shown in Fig.1. The cylinder is assumed to be excited in  $z=0$  with a unit displacement in  $z$  coordinate (that is  $u(z=0, r)=1$  and  $w(z=0, r)=0$ ), and it is free to vibrate elsewhere.

Assuming axisymmetric excitation and therefore, the response of the cylinder and harmonic dependency on time (i.e.  $e^{i\omega t}$ ), the dynamic equilibrium equation can be expressed in cylindrical coordinates  $(r, \theta, z)$  as:

$$\begin{aligned} \frac{\partial \sigma_{zz}}{\partial z} + \frac{\partial \sigma_{rz}}{\partial r} + \frac{1}{r} \sigma_{rz} &= -\rho \omega^2 u \\ \frac{\partial \sigma_{rr}}{\partial r} + \frac{\partial \sigma_{rz}}{\partial z} + \frac{1}{r} (\sigma_{rr} - \sigma_{\theta\theta}) &= -\rho \omega^2 w \end{aligned} \quad (1)$$

where  $\rho$  [kg/m<sup>3</sup>] is the material density,  $\omega$  [rad/s] is the angular frequency and  $\sigma_{rr}$ ,  $\sigma_{zz}$ ,  $\sigma_{\theta\theta}$  and  $\sigma_{rz}$  are the normal and shear components of the stress tensor. Displacement in a tangential direction can be neglected, due to the axial symmetry of the problem, meaning that no torsional vibration is present.

According to the Mindlin-Hermann (plane cross-section) theory [9], the axial and radial displacement can be defined as:

$$\begin{aligned} u(r, z) &= u_0(z) \\ w(r, z) &= r \cdot u_1(z) \end{aligned} \quad (2)$$

which correspond to the first order approximation of a power series expansion, as discussed in ref. [10].

Under such assumptions, it is straightforward to demonstrate that functions  $u_0$  and  $u_1$  can be found, by solving the following set of partial differential equations:

$$\begin{aligned} -\left(\rho \omega^2 u_0 + (\lambda + 2\mu) \frac{\partial^2 u_0}{\partial z^2}\right) - 2\lambda \frac{\partial u_1}{\partial z} &= 0 \\ 2\lambda S \frac{\partial u_0}{\partial z} - I_2 \left(\rho \omega^2 u_1 + \mu \frac{\partial^2 u_1}{\partial z^2}\right) + 4S(\lambda + \mu) u_1 &= 0 \end{aligned} \quad (3)$$

where  $S = 4\pi R^2$  is the surface area of the cross-section,  $I_2 = \pi R^4/2$  is the polar moment of inertia of the cross-section,  $\lambda$  and  $\mu$  are the lame coefficients:

$$\lambda = \frac{E\nu}{(1-2\nu)(1+\nu)} \quad \mu = \frac{E}{2(1+\nu)} \quad (4)$$

$E$  [Pa] and  $\nu$  [-] being the elastic complex modulus and Poisson's ratio, respectively.

The set of differential equations Eqs. (3) can be solved applying the boundary conditions described here above, that can be expressed in terms of function  $u_0$  and  $u_1$  as follows [10]:

$$\begin{aligned} u_0(z)\Big|_{z=0} &= 1, & u_1(z)\Big|_{z=0} &= 0 \\ \left[ (\lambda + 2\mu) \frac{\partial u_0(z)}{\partial z} + 2\lambda u_1(z) \right]_{z=L} &= 0, & \frac{\partial u_1(z)}{\partial z}\Big|_{z=L} &= 0 \end{aligned} \quad (5)$$

The reliability of the proposed analytical model will be verified against finite element simulations in Section 4A.

## 2.2. Methodology

In real experimental tests, the material is mounted on an aluminium support plate which is excited by an electromagnetic shaker, in  $z$  direction. Consequently, an imposed displacement (or velocity) is applied to the bottom side of the material while remaining surfaces are free to vibrate.

Using a logarithmic sine sweep as the excitation signal, the axial and radial velocity responses  $v_1(t)$  in  $(z, r)=(L, 0)$  and  $v_2(t)$  in  $(z, r)=(L/2, R)$  are determined using a laser vibrometer, as shown in Fig. 2.

Assuming time harmonic behaviour of the measured quantities and a unit input displacement, from the experimental tests it is possible to calculate axial and radial displacements in the frequency domain as follows:

$$\begin{aligned} U_{exp}(\omega)\Big|_{\substack{z=L \\ r=0}} &= \frac{V_1(\omega)}{j \cdot \omega} \quad [m] \\ W_{exp}(\omega)\Big|_{\substack{z=L/2 \\ r=R}} &= \frac{V_2(\omega)}{j \cdot \omega} \quad [m] \end{aligned} \quad (6)$$

where  $V_1(\omega)$ [m/s] and  $V_2(\omega)$ [m/s] are the complex frequency spectra calculated by applying a Fourier transform to velocity signals in the time domain, respectively.

In the simplest case, measurements are limited to those frequencies where all specimen dimensions are much smaller than the wavelength ( $\lambda_c$  [m]). Under such a hypothesis, the sample can be modelled by a spring [2] and in particular the axial displacement  $U$

in Eq. (6) can be considered independent from Poisson's ratio. Consequently, the measure of the axial displacement allows for the determination of the complex modulus since, as described in ref. [8]:

$$\frac{1}{V_1(\omega)} = \cos(k_c \cdot L) \square \cos\left(\sqrt{\frac{\rho\omega^2}{E}} \cdot L\right) \quad [-] \quad (7)$$

Once the Young's modulus is known, it is possible to determine Poisson's ratio by minimizing the difference between the experimental and numerical radial displacement in the frequency domain. In particular, the following cost function has been chosen for minimisation:

$$CF = \left| \sum_f \left( |W_{\text{exp}}| - |W_{\text{mod}}| \right) \right| \quad (8)$$

The minimisation procedure is based on a bounded nonlinear best-fit scheme [11] and has been implemented in Matlab®.

To summarise, starting from the experimental measurement of axial and radial displacements of an axially loaded cylindrical sample, coupled with the use of a minimisation-based approach, it is possible to determine Poisson's ratio.

### 3. MEASUREMENT SET-UP AND TESTED MATERIALS

The experimental setup for measuring the axial and radial sample response consists of a Data Physics V4 electromagnetic shaker, a B&K Type 2716C power Amplifier, a Polytec OFV 3001 laser vibrometer (sensitivity 5 mm/s/V), a PC equipped with an NI USB 4431 acquisition device and Labview® software for signal acquisition and post-processing. Moreover, a PCB 352C22 accelerometer (sensitivity 9.65 mV/g and weight 1e-3 kg) has been used to normalize velocity responses and verify the condition of unit displacement applied to the bottom side of the material. A similar calibration procedure, as described in ref. [8], between the laser vibrometer and accelerometer, has been applied in experimental tests. In particular, the sample was removed, a transfer function test was carried out and at each frequency of interest, under such conditions it was possible to calculate a correction transfer function which was applied to any successive test.

The displacement of the bottom plate has been chosen of about 0.8 μm (rms value). In addition preliminary tests were carried out increasing the displacement up to 12 μm (this was the upper limit that guarantees non-linear harmonic distortions of the shaker occurring) and no appreciable differences (lower than 0.01) in terms of Poisson's ratio

have been found.

Surely, the use of non-contact sensors for the determination of lateral and longitudinal displacement allows for a more reliable estimation of such quantities if compared with traditional uniaxial relaxation tests where usually strain gauges utilized for the measurement of lateral strain do not guarantee to avoid any disturbance of the vibration of the specimen. At the same time among possible limitations of the proposed methodology, the sliding motion of shaker could affect results since a uniaxial displacement is not guaranteed in advanced. This aspect has been investigated measuring the accelerometric response of the aluminum plate connected to the shaker on a regular grid of 16 points. In the frequency range of interest, differences lower than 0.1% have been found between all measurement points, confirming the validity of uniaxial displacement imposed to the materials.

Tests were carried out on the frequency range between 100 and 300 Hz (step 0.25 Hz) and a 10 s logarithmic sweep was used as an excitation signal. In order to avoid lateral sliding of materials during tests, they were fixed to the bottom plates using a thin adhesive layer.

Experimental tests were carried out on two open cell polymeric materials (reticulated foam and reconstituted porous rubber) commercially available for noise control applications, summarized descriptions of which can be found in Table 1. Recently, same materials have been used for the investigation in terms of acoustical and pore structure properties<sup>12</sup>. The mechanical behaviour of poroelastic media has been widely investigated in literature<sup>4,13</sup>. The main assumption is that the fluid phase of the porous material is usually assumed to play a negligible role in the low-frequency range (typically frequencies below 50 Hz) so that the material can be considered in “in vacuum” conditions. At higher frequencies, although Biot’s model requires the use of mechanical parameters of the porous skeleton “in vacuum”, a real measurement of these parameters in vacuum conditions can induce some difficulties. For example, the reduction of temperature of the porous frame in vacuum may change the properties of the frame or the vacuum conditions may destroy the skeleton of some porous foams. In order to overcome these limitations, tests are carried out under ambient conditions and the porous medium is considered for small deformations a linear viscoelastic material. The same assumption has been made for the tests of materials presented in this research. Fig. (3) depicts the real part of the complex modulus and the damping loss factor for both materials calculated using Eq. (7). In order to verify the condition  $2R \ll \lambda_c$ , the longitudinal wavelength for both materials was determined, using the direct

measurement of complex wave number (Eq. (7)). A comparison of test sample wavelength and diameter is depicted in Fig. (4).

## 4. RESULTS

In order to investigate the capability of the proposed analytical method (Eqs. 7-9) of correctly determining the axial and radial displacement of a cylindrical specimen, a series of preliminary finite element model (FEM) simulations were carried out and results in terms of amplitude of axial and radial displacements have been compared to those obtained using the proposed methodology (Fig. 5). The values of mechanical and geometrical properties of simulated samples S1-S3 are summarized in Table 2. Finite element simulations were run using a commercial software, where the solid has been modeled with quadratic tetrahedron elements (using the criterion of ten elements per wavelength). The linear systems were solved using the Multifrontal Massively Parallel Sparse (MUMPS) direct solver, already implemented in the software.

From the comparisons in Fig. (5), it is possible to observe a satisfying agreement between FEM and analytical simulations, both for radial and axial displacements. Furthermore, the hypothesis of weak dependency of axial displacement from Poisson's ratio has been validated, using the finite element model described above. In particular, simulations on samples S1-S3 have been repeated, varying the Poisson ratio between 0 and 0.45. It has been found that the relative deviation in both real and imaginary parts of axial displacement  $U(\omega)$  was lower than 1%, while the relative deviation for radial displacement  $W(\omega)$  was approximately 50% for any frequency and configuration. On the one hand, such results confirm the validity of the assumption on axial displacement, and on the other hand, the strong dependency of radial displacement on Poisson's ratio. The assumption of validity of the proposed methodology at frequencies where specimen dimensions are lower than longitudinal wavelength, were validated by running a FEM simulation on sample S2 in the frequency range between 2000 Hz and 3000 Hz. Although the value of Poisson's ratio determined using the analytical approach (0.17) is comparable to the one fixed as an input value (0.2 in Table 2), the comparison between finite element model and analytical solution, in terms of amplitude of both axial and radial displacements, cannot be considered satisfactory, as depicted in Fig. 6.

The proposed methodology has been preliminary validated by utilizing numerical data of radial displacement for samples S1-S3. The comparison of Poisson's ratio from the proposed method to input data of the FEM models are reported in Table 3.

Successively, the proposed methodology was applied to materials A and B in order to estimate their Poisson's ratio. Each material was also tested by using a quasi-static method [14], and results are summarized in Table 3. A satisfactory level of reliability of proposed methodology for the determination of the Poisson's ratio was observed in all examined cases, with a maximum deviation of 0.02. Figures 7 and 8 show the comparison between experimental test and analytical model for radial displacement, once Poisson's ratio has been determined using the proposed methodology. The finite element method results are depicted for both materials in the same graphs. A satisfactory comparison between the experimental and numerical radial displacement can be seen in the figures.

Lastly, sensitivity analysis was carried out on radial displacement for materials A and B. In particular, for each material, analytical model results with different Poisson's ratio have been plotted against experimental data, and in all cases an accurate dependency of radial displacement on the Poisson's ratio can be observed, determined by using the proposed approach (Fig. 9).

## 5. CONCLUSIONS

This paper has presented and discussed a novel method for determining the Poisson's ratio value of homogeneous and isotropic viscoelastic materials, by using a simplified plane cross-section (Mindlin-Hermann) theory for axial and radial displacement, when the sample is axially excited. Analytical model reliability has been positively validated against a finite element. The results of the proposed methodology from two different materials were compared to data from well-established quasi-static data and the comparison can be considered to be satisfactory.

## REFERENCES

1. N.W. Tschoegl, W.G. Knauss, I. Emri, Poisson's ratio in linear viscoelasticity-a critical review, *Mechanics of Time-Dependent Materials* 6 3–51(2002).
2. T. Pritz, Measurement methods of complex Poisson's ratio of viscoelastic materials, *Applied Acoustics* 60 279-292 (2000).
3. W. Warren, and A. Kraynik, The linear elastic properties of opencell foams, *J. Appl. Mech.* 55, 341–346 (1988).
4. E. Mariez, S. Sahraoui, J. F. Allard, Elastic constants of polyurethane foam's skeleton for Biot model, in *Internoise 96*, Liverpool, Great Britain, pp. 951–954 (1996).
5. L. Jaouen, A. Renault, M. Deverge, Elastic and damping characterizations of acoustical

- porous materials: Available experimental methods and applications to a melamine foam, *Applied Acoustics* **69–12** 1129–1140 (2008).
- 6. R. H. Pritchard, P. Lava, D. Debruyne and E. M. Terentjev, Precise determination of the Poisson ratio in soft materials with 2D digital image correlation, *Soft Matter* 9-26 6037-6045 (2013).
  - 7. J. E. Zorzi, and C. A. Perottoni, Estimating Young's modulus and Poisson's ratio by instrumented indentation test. *Materials Science and Engineering: A* 574: 25-30 (2013).
  - 8. P. Bonfiglio, F. Pompoli, K.H. Horoshenkov, M. I. B. S. A. Rahim, A simplified transfer matrix approach for the determination of the complex modulus of viscoelastic materials, *Polymer Testing* 53 180-187(2016).
  - 9. M. Shatalov, I. Fedotov, J. Marais, M. D. Tenkam, Longitudinal vibration of isotropic solid rods: from classical to modern theories. INTECH Open Access Publisher (2011).
  - 10. D.D. Ebenezera, K. Ravichandran, C. Padmanabhan, Forced vibrations of solid elastic cylinders, *Journal of Sound and Vibration* 282 991–1007 (2005).
  - 11. J.C. Lagarias, J.A. Reeds, M.H. Wright, P.E. Wright, Convergence properties of the Nelder-Mead simplex method in low dimensions, *SIAM J. Optim.* 9 (1) 112-147 (1998).
  - 12. F. Pompoli, P. Bonfiglio, K.V. Horoshenkov *et al.*, How reproducible is the acoustical characterization of porous media? *J. Acoust. Soc. Am.* 141 (2) 945-955 (2017).
  - 13. O. Danilov, F. Sgard, X. Olny, On the limits of an “in vacuum” model to determine the mechanical parameters of isotropic poroelastic materials, *Journal of Sound and Vibration* 276 729–754 (2004).
  - 14. P. Bonfiglio, F. Pompoli, P. Shravage, Quasi-static evaluation of mechanical properties of poroelastic materials: static and dynamic strain dependence and in vacuum tests, In: *Proceeding of Acoustics 08* pp 29–34, Paris (2008).

Figure 1 – A solid cylinder of length  $L$  and radius  $R$ .  $u$  and  $w$  are the axial and radial components of displacement, respectively.

Figure 2 – Measurement layout.

Figure 3 – Materials A and B. (a) Real part of the complex modulus, (b) damping loss factor.

Figure 4 – Comparison between wavelength and diameter for both tested materials.

Figure 5 – Validation of analytical model.

Figure 6 – Amplitude of axial and radial displacements at high frequencies. Comparison between finite element model and proposed methodology for sample S2.

Figure 7 – Radial displacement form material A: (a) Real part, (b) Imaginary part, (c) Amplitude.

Figure 8 – Radial displacement form material B: (a) Real part, (b) Imaginary part, (c) Amplitude.

Figure 9 – Sensitivity analysis on materials A and B.

**Table 1. Description of tested materials.**

Material	A	B
Description	Reconstituted porous rubber (open cells)	Reticulated foam (open cells)
Density [kg/m <sup>3</sup> ]	325	10
Thickness [mm]	25	24
Diameter [mm]	45	45

**Table 2. Description of simulated materials.**

Material	S1	S2	S3
Real part of the complex modulus [Pa]	1e5	1e6	1e7
Poisson's ratio [-]	0.05	0.2	0.4
Damping loss factor [-]	0.05	0.2	0.5
Density [kg/m <sup>3</sup> ]	10	100	300
Thickness [mm]		25	
Diameter [mm]		45	

**Table 3. Poisson's ratio of simulated and tested materials.**

Material	FEM / Quasi-static method	Proposed methodology
S1	0.05	0.05
S2	0.2	0.21
S3	0.4	0.42
A	<b>0.05</b>	0.05
B	<b>0.21</b>	0.20

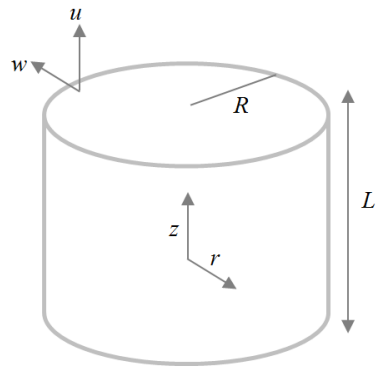


**Figure 1 - A solid cylinder of length  $L$  and radius  $R$ .  $u$  and  $w$  are the axial and radial components of displacement, respectively.**

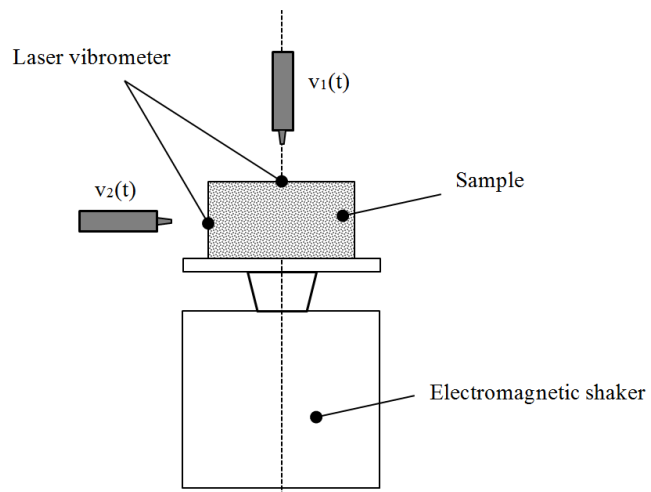


**Figure 2 – Measurement lay-out.**

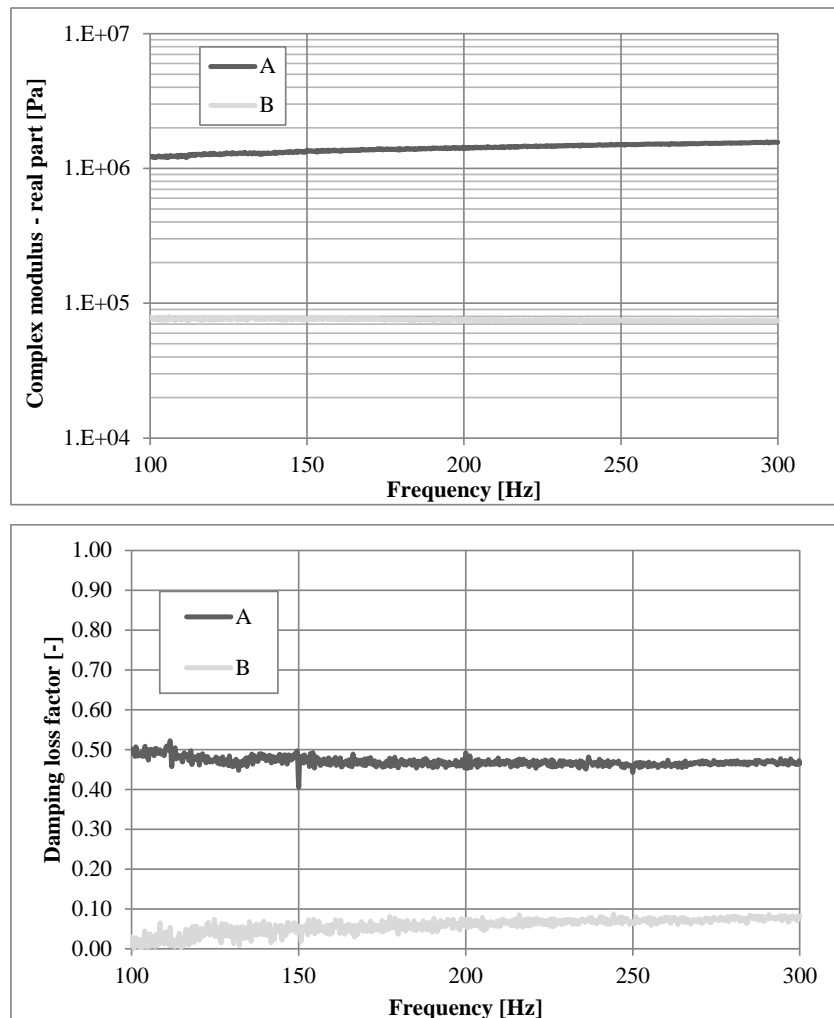


**Figure 3 – Materials A and B. (a) Real part of the complex modulus, (b) damping loss factor.**

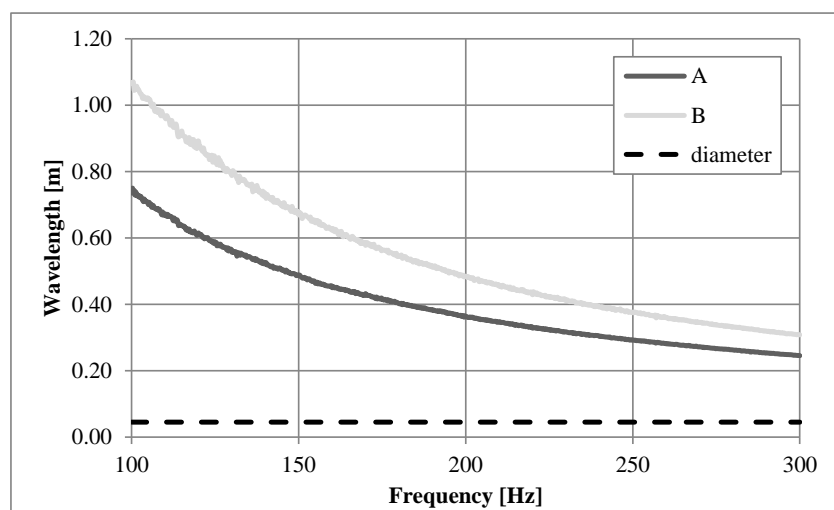


**Figure 4 – Comparison between wavelength and diameter for both tested materials.**

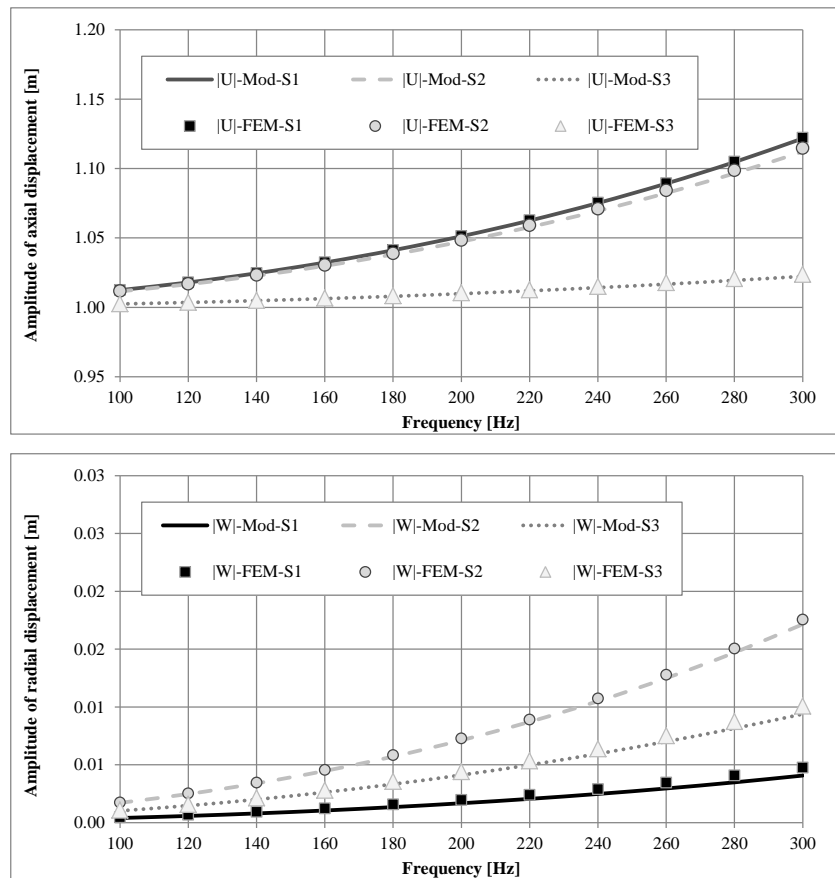


Figure 5 – Validation of the analytical model.

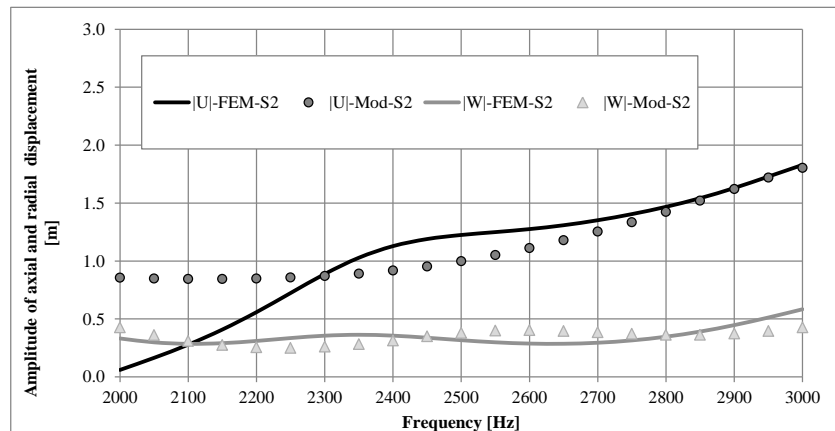
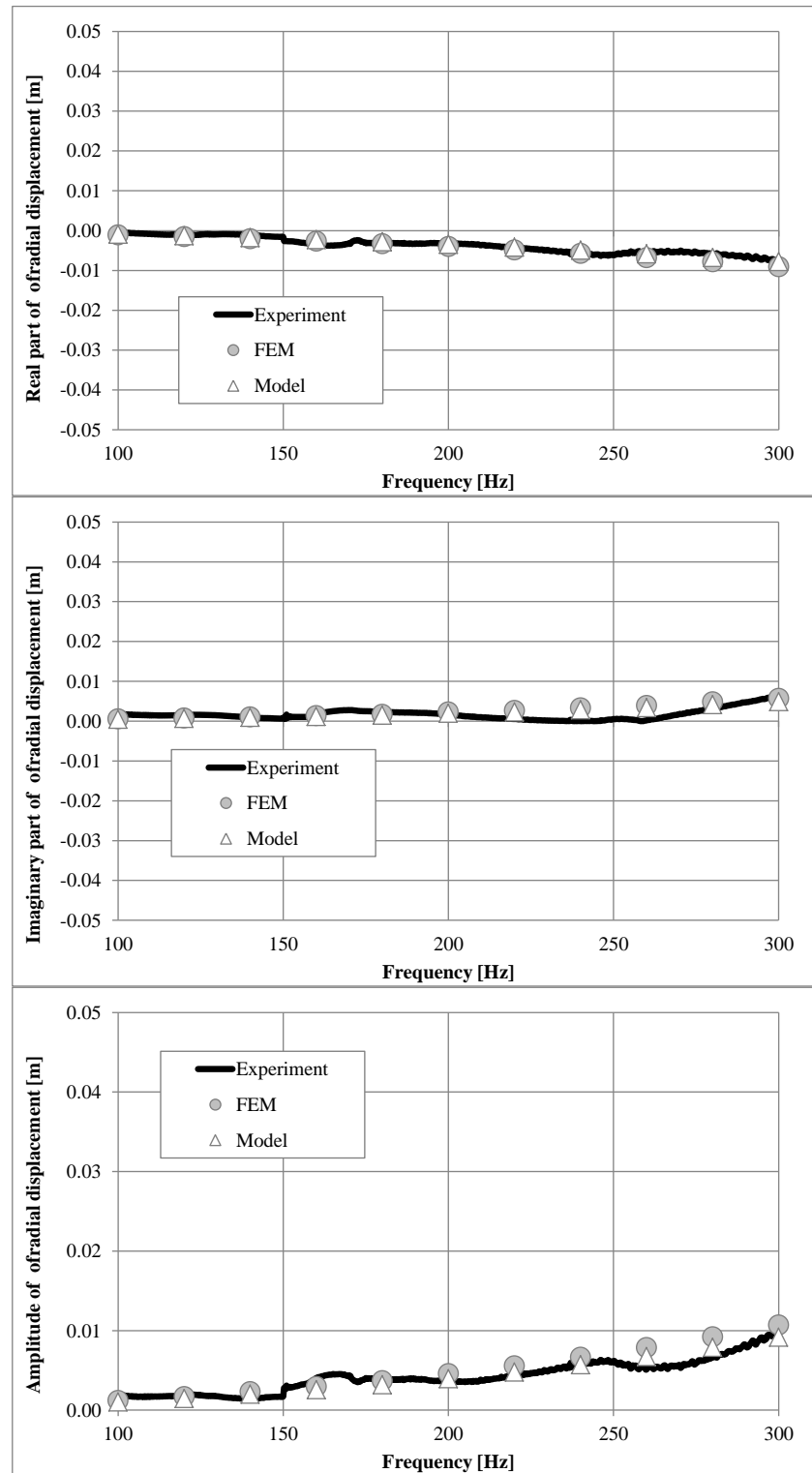
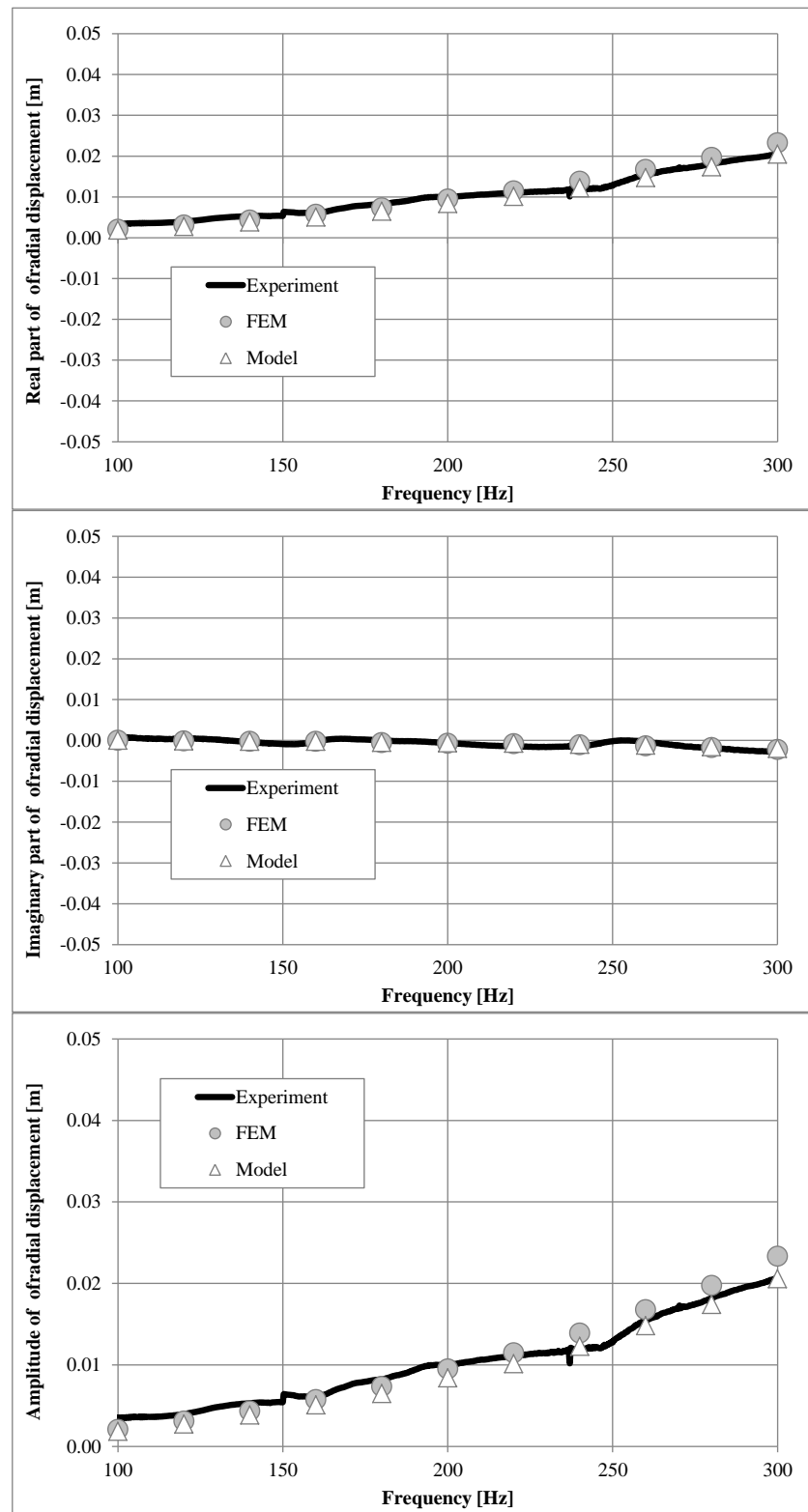


Figure 6 – Amplitude of axial and radial displacements at high frequencies. Comparison between finite element model and proposed methodology for sample S2.



**Figure 7 – Radial displacement form material A: (a) Real part, (b) Imaginary part, (c) Amplitude.**



**Figure 8 – Radial displacement form material B: (a) Real part, (b) Imaginary part, (c) Amplitude.**

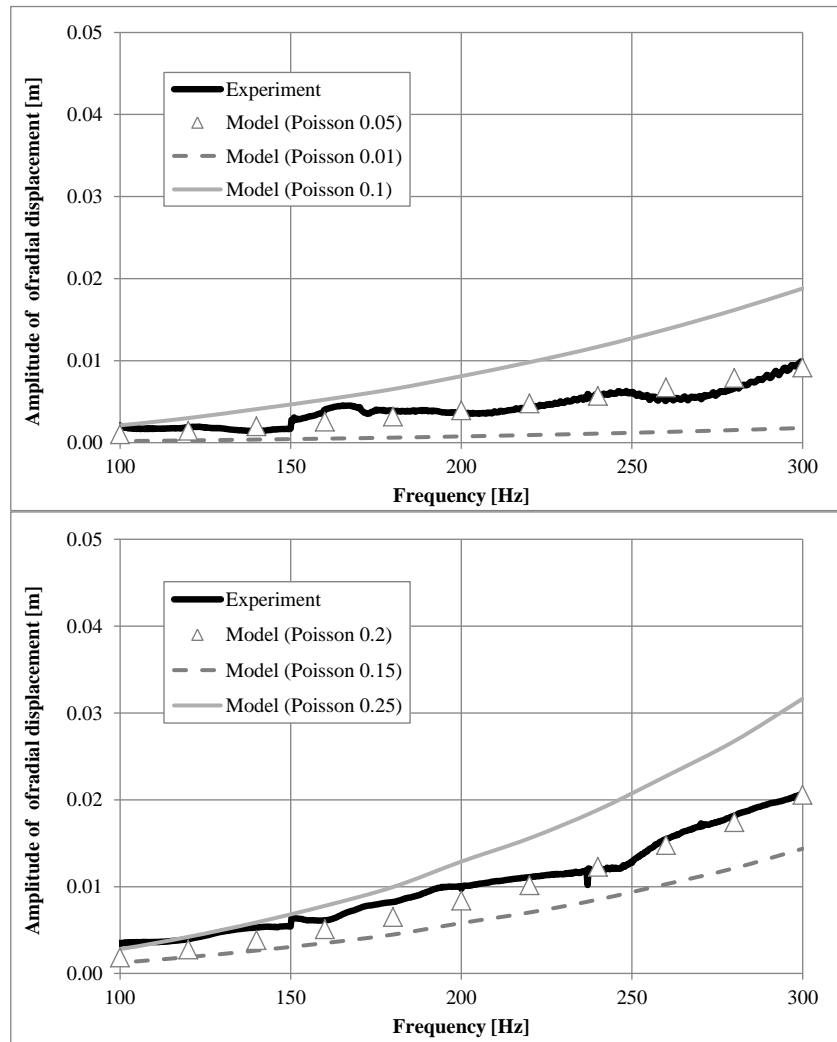


Figure 9 – Sensitivity analysis on materials A and B.